Eur. Phys. J. D **41**, 143–150 (2007)
DOI: 10.1140/epjd/e2006-00187-x

THE EUROPEAN PHYSICAL JOURNAL D

Excessive Doppler broadening of the H_α line in a hollow cathode glow discharge

Radial distribution, influence of surface coverage and temperature effect

N.M. Šišović[1], G.Lj. Majstorović[2], and N. Konjević[1,a]

[1] Faculty of Physics, University of Belgrade, P.O. Box 368, 11001 Belgrade, Serbia
[2] Military Academy, Pavla Jurišića – Šturma 33, 11105 Belgrade, Serbia

Received 27 April 2006 / Received in final form 4 July 2006
Published online 18 August 2006 –

Abstract. A comparative study of the radial intensity distribution of the excessively Doppler broadened hydrogen H_α line in a hollow cathode (HC) glow discharge operated in hydrogen and argon-hydrogen gas mixtures with stainless steel (SS) and titanium (Ti) cathode is reported. The main interest of this work is focused on the dependence of radial distribution upon cathode material and cathode surface composition. The analysis of experimental radial distributions and results obtained from $H^+ \rightarrow$ metal surface interaction simulation combined with available data for H → metal target interaction explains the difference between SS and Ti cathodes. These results explain also the important role of metal hydrides at the cathode surface for discharge-HC interaction. The influence of the hollow cathode temperature on the radial distribution of the excessively broadened H_α line and on the emission of Ar I and Ar II lines from discharge in argon-hydrogen gas mixture are also investigated. The increase of the excessive Doppler broadened part of the H_α line profile with HC temperature is always detected. The intensity of Ar I and Ar II lines is also used to examine the influence of small admixtures of hydrogen in argon.

PACS. 32.30.Jc Visible and ultraviolet spectra – 32.70-n Intensities and shapes of atomic spectral lines – 52.80.Hc Glow; corona – 52.70.Kz Optical (ultraviolet, visible, infrared) measurements – 52.20.Hv Atomic, molecular, ion, and heavy-particle collisions – 52.40.Hf Plasma-material interactions; boundary layer effects

1 Introduction

It has been demonstrated recently that the excessive Doppler broadening (EDB) of hydrogen Balmer lines may be used for discharge-cathode surface interaction monitoring [1]. The shape of these lines emitted from some low-pressure gas discharges operated with hydrogen isotopes or hydrogen gas mixtures with inert gases exhibits unusual multi component behavior, see e.g. Figures 1a and 1b. The same EDB shapes of H_α and H_β lines are detected in a plane cathode glow discharge operated with N_2–H_2 gas mixture [2]. The origin of the narrowest part of the profile in Figure 1a is related to the Doppler broadening of the thermalized excited hydrogen atoms H^* in the negative glow region of the discharge. The broader middle part of the line profile is related to excited hydrogen atoms generated in electron collisions with H_2. The pedestal of the line profile is very broad indicating that energetic excited hydrogen atoms having energies larger than hundreds of electron volts are generated in the discharge. The presence of large energy excited hydrogen atoms implies that fast hydrogen atoms H_f of higher energy exist in the discharge [3]. As pointed out already, the origin of the narrow- and medium-width part of the line profile may be explained on the basis of well-established processes.

The primary explanation of the broadest part-pedestal of the line profile comes from the sheath-collision model. In this model ions H^+ and H_3^+ are accelerated in a high-voltage discharge sheath and produce fast H atoms in charge transfer/dissociation collisions with the matrix gas–molecular hydrogen. The fast H atoms are then excited and scattered in another collision. The same excitation process is occurring with H atoms backscattered from the cathode [4–6]. In the Ar–H_2 discharge, see the H_α profile in Figure 1b, the contribution of H^+ ion is negligible in comparison with that of H_3^+ ion, see e.g. [4,7]. The latter ions fragment in collisions with matrix gas or at the cathode surface generating H_f atoms of lower energy, and consequently lower energy excited atoms H^* are produced.

Another model of EDB has been proposed by Mills et al., see e.g. [8,9]. According to this model, in the resonance transfer (RT) process H atoms react with certain ions, for instance He^+, Ar^+ or other "resonance catalysts"

[a] e-mail: nikruz@ff.bg.ac.yu

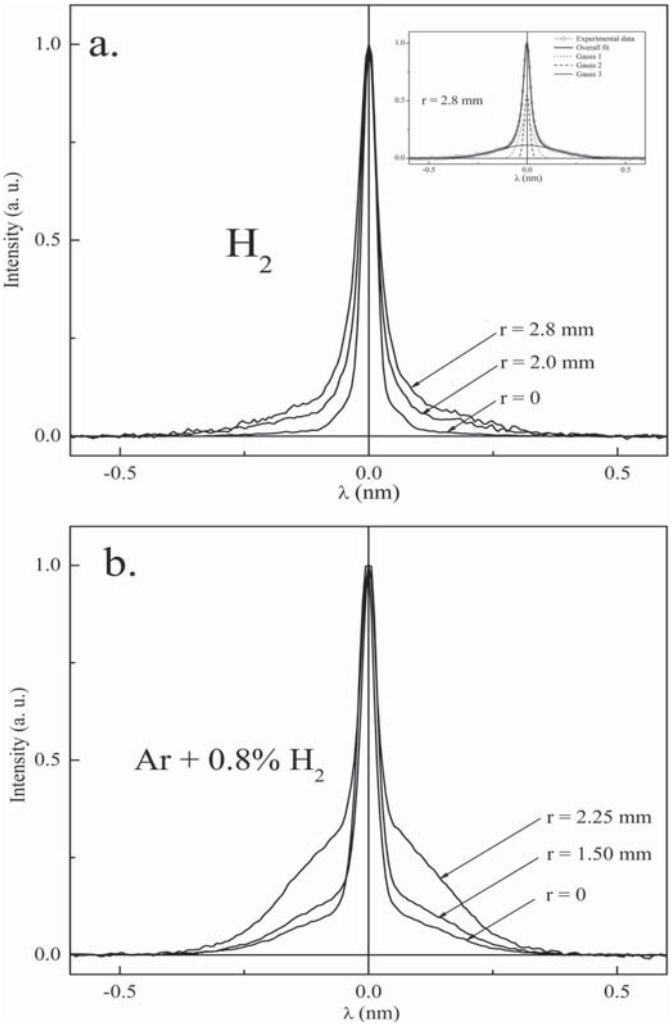

Fig. 1. Typical H_α profiles recorded at different radial positions in: (a) stainless steel hollow cathode; upper right corner depicts the H_α line shape at radial position $r = 2.8$ mm fitted with three Gaussians; and (b) titanium hollow cathode. Discharge conditions: (a) pure H_2 at $p = 4$ mbar; $I = 90$ mA; $U = 427$ V and $T_{wall} = 74$ °C; (b) Ar–H_2 mixture at $p = 4$ mbar; $I = 90$ mA; $U = 338$ V and $T_{wall} = 75$ °C.

produced by the electric discharge, to generate excess energy. The RT process is followed by excessive Doppler broadening of the hydrogen Balmer lines, which according to references [8,9] reveals the presence of high energy excited hydrogen atoms-carriers of excess energy produced in the RT process. Recently, Phelps [10,11] reported a thorough comparative analysis of Mills and co-workers RT experiments and most of the other EDB Balmer line studies. On the bases of this analysis and the fact that Mills and co-workers [8,9] do not provide a set of elementary processes with cross-sections for converting the energy of RT products into the fast excited hydrogen atoms, one may conclude that RT model cannot be used to explain EDB of hydrogen Balmer lines. On the other hand, a number of experiments disagree with RT model predictions, see e.g. [10,11] and references therein. Therefore, the sheath-collision model will be used throughout this study for the interpretation of EDB results.

The experiment in reference [1] was carried out using hollow cathode (HC) discharges observed end-on without attempting to achieve any spatial resolution of the EDB of the Balmer lines. The work presented here is an extension of these earlier studies [1,12] with an emphasis on the radial distribution of the EDB behavior of the H_α line in HC discharge in H_2 and Ar–H_2 mixtures. The influence of HC temperature and small admixtures of hydrogen in Ar on the Ar I and Ar II line emission is also studied.

2 Experimental

The hollow cathode glow discharge (HCGD) source with two symmetrically positioned kovar anodes and titanium (Ti) or stainless steel 10/80 (SS) cathode is used as a discharge source. The HC tubes were 100 mm long with 6 mm internal diameter and 1 mm wall thickness. When operated with pure hydrogen, the discharge filled approximately one half of the SS or Ti HC length, starting from the side of the anode used. In the case where Ar–H_2 gas mixture is used, the discharge filled the whole volume of the HC. The construction details of the HC discharge source are described elsewhere [12]. The only difference is the cathode–anode distance, which was on one side 20 mm, and 15 mm on the other. In this way the discharge voltage can be changed using one or the other anode.

All HCGD experiments were carried out with hydrogen (purity of 99.999%) and Ar–H_2 (Ar + 0.8%H_2) provided by Messer-Tehnogas, Serbia. The continuous flow of H_2 and gas mixture was 60 cm^3/min and 16 cm^3/min (at room temperature and atmospheric pressure), respectively. The working gas was sustained at pressures in the range 3–5 mbar by means of a needle valve and two-stage mechanical vacuum pump. To prevent oil vapor back streaming from the vacuum pump, a zeolite trap is placed between the discharge chamber and the pump. The gas pressure measurements are performed on both sides of the discharge tube with standard U-shaped oil manometers. The difference of gas pressure between the gas inlet and outlet from the discharge tube was about 30% during discharge operation. Within the experimental scatter, spectroscopic recordings do not show difference between measurements performed from the gas inlet or outlet side. The results of reported gas pressure measurements represent an average value between gas inlet and outlet values.

To operate the discharge in a DC mode, a current stabilized power supply (Kepco BHK2000-0.1M, 0–2 kV, 0–100 mA) is used. An air-cooled variable 10 kΩ ballast resistor is placed in series with the discharge and power supply. For all measurements, the cathode was grounded.

During the discharge operation, the cathode was either air cooled with a fan (110 mm dia; AC 220V/13W), placed 150 mm from the discharge tube, or gradually heated by changing the cooling rate of the fan. The temperature of the outer wall of the HC tube is measured by a K-type thermocouple.

Table 1. Experimental conditions, relative contributions G_i/G_{total} $(i = 1, 2, 3)$ and energies E_i $(i = 1, 2, 3)$ of excited hydrogen atoms obtained by applying three Gaussian fit to the H_α profiles for stainless steel hollow cathode glow discharge in pure H_2 at $p = 4$ mbar; $I = 90$ mA; r denotes radial position.

						hydrogen atom energy		
Temperature (°C)	Voltage (V)	r (mm)	G_1/G_{total} (%)	G_2/G_{total} (%)	G_3/G_{total} (%)	E_1 (eV)	E_2 (eV)	E_3 (eV)
74	427	0	61.3	25.6	13.1	0.3	5	59
		0.8	60.2	26.0	13.8			
		1.2	56.2	25.7	18.1		4	
		2.0	42.5	28.6	28.9			
		2.8	16.8	31.7	51.5		3	
100	438	0	57.7	28.5	13.8	0.3	5	59
		0.8	55.7	29.1	15.2			
		1.2	48.0	30.8	21.2		4	
		2.0	30.8	36.4	32.8		3	
135	443	0	56.3	28.3	15.4	0.3	5	59
		0.8	54.5	29.6	15.9			
		1.2	49.4	29.8	20.8		4	
		2.0	29.6	37.3	33.1		3	

Table 2. Same as for Table 1, but for glow discharge in argon-hydrogen mixture at $p = 4$ mbar; $I = 90$ mA.

						hydrogen atom energy		
Temperature (°C)	Voltage (V)	r (mm)	G_1/G_{total} (%)	G_2/G_{total} (%)	G_3/G_{total} (%)	E_1 (eV)	E_2 (eV)	E_3 (eV)
55	300	0	10.6	17.2	72.2	0.3	1	36
		0.75	7.5	12.0	80.5			
		1.50	3.8	4.6	91.6			
		2.25	1.3	2.0	96.7			
100	308	0	8.4	16.1	75.5	0.3	1	36
		0.75	6.6	10.5	82.9			
		1.50	3.6	3.7	92.7			
		2.25	1.2	2.0	96.8			
135	315	0	5.0	10.3	84.7	0.3	1	36
		0.75	4.1	6.6	89.3			
		1.50	2.3	2.3	95.4			
		2.25	0.5	2.3	97.2			

The radial distribution spectra recordings were performed with unity magnification in equidistant steps perpendicular to the discharge axis, with an estimated spatial resolution of 0.25 mm or 0.40 mm. For radial intensity measurements the discharge was run between HC and rear anode, located at 20 mm from the cathode. The results of test measurements using front or rear anode did not show a difference within experimental uncertainty. The light from the discharge was focused with an achromatic lens (focal length 75.8 mm) onto the entrance slit of a Carl Zeiss PGS-2 spectrometer (2 m focal length; reciprocal dispersion of 0.74 nm/mm with 651 g/mm reflection grating in first diffraction order). All spectral measurements were performed with an instrumental profile very close to Gaussian with measured full half-width of 0.018 nm. Signals from CCD detector (Toshiba 1304USB, 29.1mm, 3648 channels) are A/D converted, collected and processed by PC.

3 Results and discussion

Three H_α line profiles recorded at various radial positions from the axis of HCGD operated with SS cathode in H_2 are presented in Figure 1a. In the upper right corner of this figure the experimental H_α profile recorded at the radial position $r = 2.8$ mm and the best fit with three Gaussians are presented. The area of each Gaussian, G_1, G_2 and G_3, represents the contribution of a group of excited hydrogen atoms whose origin is discussed in the introduction. Experimental conditions, relative contributions G_i/G_{total} $(i = 1, 2, 3)$ and energies E_i $(i = 1, 2, 3)$ of excited hydrogen atoms obtained by fitting the H_α profiles for all considered cases are given in Tables 1–4. Depending upon radial position and the relative contribution of G_3 to the overall profile, the estimated uncertainty of E_3 values in Tables 1–4 varies from 2–5 % in hydrogen and from 0.5–2% in Ar–H_2 gas mixture.

Table 3. Experimental conditions, relative contributions G_i/G_{total} $(i = 1, 2, 3)$ and energies E_i $(i = 1, 2, 3)$ of excited hydrogen atoms obtained by applying three Gaussian fit to the H_α profiles for titanium hollow cathode glow discharge in pure H_2 at $p = 4$ mbar; $I = 90$ mA; r denotes radial position.

						hydrogen atom energy		
Temperature (°C)	Voltage (V)	r (mm)	G_1/G_{total} (%)	G_2/G_{total} (%)	G_3/G_{total} (%)	E_1 (eV)	E_2 (eV)	E_3 (eV)
74	424	0	71.4	22.3	6.3	0.3	5	50
		0.75	65.4	23.7	10.9		4	
		1.50	48.4	29.6	21.9			
		2.25	33.6	38.9	27.5		3	
100	435	0	66.5	25.3	8.2	0.3	5	50
		0.75	59.8	27.0	13.2		4	
		1.50	39.6	35.8	24.6			
		2.25	20.9	42.9	36.2		3	
125	448	0	65.7	25.2	9.1	0.3	5	50
		0.75	59.5	27.6	12.9		4	
		1.50	42.0	34.0	24.0			
		2.25	19.3	44.7	36.0		3	

Table 4. Same as for Table 3, but for glow discharge in argon-hydrogen mixture at $p = 4$ mbar; $I = 90$ mA.

						hydrogen atom energy		
Temperature (°C)	Voltage (V)	r (mm)	G_1/G_{total} (%)	G_2/G_{total} (%)	G_3/G_{total} (%)	E_1 (eV)	E_2 (eV)	E_3 (eV)
75	338	0	19.0	31.0	51.0	0.3	1	37
		0.75	218.2	31.0	50.8			
		1.50	14.6	23.6	61.8			
		2.25	6.2	12.2	81.6			
100	336	0	14.8	28.7	56.5	0.3	1	37
		0.75	16.9	26.7	56.4			
		1.50	10.5	18.2	71.3			
		2.25	4.9	8.5	86.6			
135	340	0	15.1	20.0	64.9	0.3	1	37
		0.75	12.1	21.9	65.9			
		1.50	8.9	13.9	77.1			
		2.25	4.4	6.8	88.9			

The main subject of our interest is the broadest Gaussian G_3, which is related to EDB and proportional to the number of fast excited atoms emitting the H_α line. Before one starts to discuss and compare results obtained in this study with different hollow cathode discharges it is necessary to note that the HC temperature variation is associated with a change of discharge voltage U. By analyzing data in Tables 1–4, one may conclude that the change of voltage in the studied range of temperature is 10% at the most. This difference of U does not produce noticeable change of E_3 values expected as a consequence of sheath potential variation, see Tables 1–4. From these tables it is evident also that G_3 contributions change in the range 15% to 40% for the same span of T. This suggests that HC temperature plays a more important role than discharge voltage.

Three typical H_α profiles recorded in Ar–H_2 gas mixture at various radial positions of Ti HC are given in Figure 1b. As always, in Ar–H_2 mixtures, the profiles have considerably larger contribution of G_3, but the same trend of increasing G_3 in respect to central narrower part of line profile remains, see Figure 1b. Since G_3 contribution becomes larger close to the cathode surface, the overall profile in Ar–H_2 mixture looks much broader.

The shape of the H_α line profiles for SS HC in Figure 1a are in good agreement with those recorded in a plane cathode glow discharge in hydrogen, see Figure 2 in [13]: profiles recorded at different distances from the iron cathode show the same tendency of increasing G_3 in the vicinity of cathode. Even more, three Gaussian fits match the H_α profile recorded at the position of 0.5 mm from iron cathode surface [13] at a confidence level of 0.05, giving relative contribution G_3/G_{total} of 56%. In this study, the corresponding G_3 contribution of 51.5% is determined at the position 0.2 mm from the SS HC surface, see Table 1.

Radial distribution of the H_α line intensity and G_1, G_2 and G_3 line intensity contributions for SS and Ti HCGD are given in Figures 2 and 3, respectively. The elementary processes responsible for the excitation of H atoms, contributing to G_1 and G_2 component of the H_α line profile, are dependent primarily upon electron density N_e and electron energy. In our high-pressure low-voltage

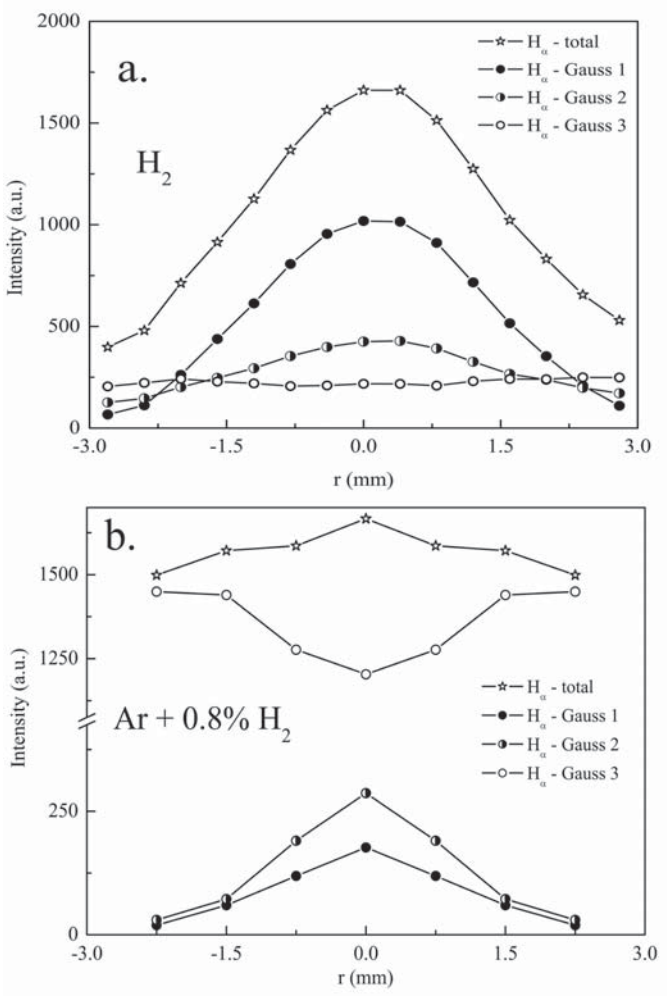

Fig. 2. The intensity distribution of the H_α spectral line and its Gaussian components vs. radial coordinate r. Experimental conditions: stainless steel hollow cathode discharge in (a) pure H_2 at $p = 4$ mbar; $I = 90$ mA; $U = 427$ V and $T_{wall} = 74$ °C; (b) Ar–H_2 mixture at $p = 4$ mbar; $I = 90$ mA; $U = 300$ V and $T_{wall} = 55$ °C.

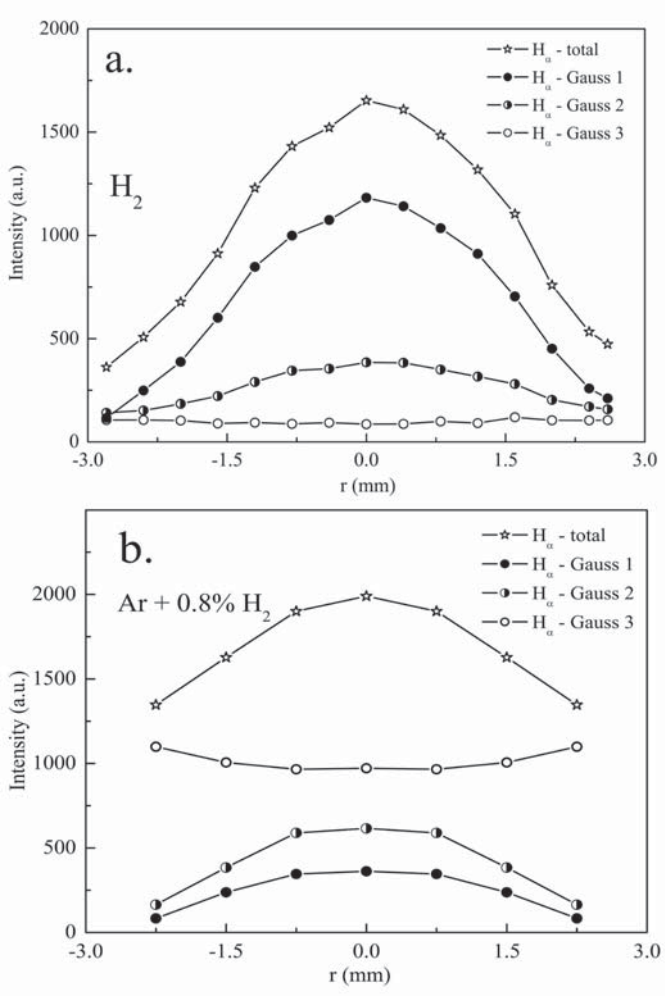

Fig. 3. The intensity distribution of the H_α spectral line and its Gaussian components vs. radial coordinate r. Experimental conditions: titanium hollow cathode discharge in (a) pure H_2 at $p = 4$ mbar; $I = 90$ mA; $U = 424$ V and $T_{wall} = 75$ °C; (b) Ar–H_2 mixture at $p = 4$ mbar; $I = 90$ mA; $U = 338$ V and $T_{wall} = 75$ °C.

HCGD with relatively high current, both these parameters increase from the surface towards the axis of HC. Best proof for this statement is a bell shape radial intensity distribution of the Ar I and Ar II lines, see below.

With both HC operated in pure H_2, the radial distribution of the G_3 component is flat and therefore the overall profile has a bell shape, see Figures 2a and 3a. In order to explain the difference between G_3 contributions for HCGD with SS and Ti cathodes, see Tables 1–4, the number R_N and the energy R_E coefficients for incident H^+ ions are calculated first for clean metal surface and than for surfaces covered with metal hydride layers, see Table 5. For this purpose we have utilized a FORTRAN subroutine [14] which implements a code described by Tabata and Ito [15]. This is not the only process of interaction between energetic particles and the cathode surface. The fast hydrogen atoms H_f, resulting from collisions of fast H^+ and H_3^+ ions with H_2, are also back scattered from the cathode surface. To analyze this process the results of a simulation with Fe and Ti targets using the binary collision cascade program MARLOWE [16] are used. Both sets of results for R_N and R_E, see Table 5, and [16], show that the fraction of particles and energy reflected decreases with increasing hydrogen content of the metal hydride. Furthermore, both scattering coefficients are larger for Fe (very close to SS) than for Ti, see also Table 5 and [16]. For this reason the energy of excited hydrogen atoms (half-width of G_3 in energy units), see Tables 1 and 3, is larger for SS ($E_3 = 59$ eV) than for Ti HC ($E_3 = 50$ eV), in spite of similar voltage for both discharges.

Thus, the results of both simulations, from Table 5 and [16], for Fe or SS and for Ti are in qualitative agreement with G_3 values (proportional to R_N and R_E) and their temperature trend in Tables 1 and 3. The increase of G_3 contribution versus temperature may be related to the decrease of the metal hydride layer with an increase of

Table 5. The number R_N and energy R_E back-scattering coefficients for pure metal and surface with metal hydride versus energy of H^+ ions calculated using simulation program [14] with a code published in [15].

Hydrogen ion	Fe		H:Fe = 1		H:Fe = 2		Ti		H:Ti = 1		H:Ti = 2	
energy (eV)	R_N	R_E	R_E	R_N	R_E	R_N	R_E	R_N	R_E	R_N	R_E	R_N
100	0.48	0.28	0.20	0.11	0.13	0.07	0.35	0.20	0.17	0.09	0.12	0.06
200	0.43	0.23	0.20	0.10	0.13	0.06	0.31	0.16	0.16	0.08	0.11	0.05
300	0.39	0.20	0.19	0.09	0.13	0.05	0.28	0.14	0.15	0.07	0.11	0.04
400	0.36	0.18	0.19	0.08	0.13	0.05	0.25	0.12	0.15	0.06	0.10	0.04
500	0.34	0.16	0.18	0.08	0.12	0.05	0.24	0.11	0.14	0.05	0.10	0.04

HC temperature. It should be noticed that in this analysis, due to the lack of relevant data, the interaction of fast H_3^+ ions with the cathode and their contribution to G_3 is neglected. The interaction of H_3^+ includes processes of collisions with the matrix gas, neutralization at the cathode, fragmentation and back-scattering of fast H atoms from the cathode surface. It seems, however, that the omission of the H_3^+ role in G_3 behavior does not change conclusion drawn from analysis of H^+ and H_f interaction with the cathode. Namely, if one makes comparison of G_3 values in Tables 2 and 4 for HCGD run in Ar–H_2 gas mixture, where the H_3^+ ions are prevailing, larger G_3 values are detected for SS again. On the other hand, the G_3 temperature trend for the Ar–H_2 discharge is rising, likewise in the pure H_2 case, for both HC materials. These results may, in part, justify the neglect of H_3^+ ion in the explanation of G_3 temperature trend in pure H_2. Apart from the magnitude of G_3, the only difference between HCGD operated in H_2 and Ar–H_2 is the half width of the G_3 component which is, due to the fragmentation of H_3^+, systematically smaller, see Tables 2 and 4.

The secondary emission processes, which can affect the sheath field profile, and consequently the ion acceleration, are neglected in our analysis of discharge-surface interaction. This is due to the lack of secondary emission coefficients data for SS and Ti surfaces covered with a hydride layer having variable hydrogen/metal ratio.

In the Ar–H_2 mixture, both G_3 radial distributions show minima around the HC axis, but due to G_1 and G_2 profiles, the overall radial H_α distribution has a maximum value at the HC axis, see Figures 2b and 3b. Here, one should comment first on the difference between G_3 values in HCGD operated with Ar–H_2 mixture with SS cathode reported in [1] and results in Table 2. Under similar discharge conditions and HC temperature 120 °C, $G_3 = 0.91$ [1], while in Table 2 for a temperature of 100 °C, G_3 changes from 0.76 at the axis to 0.97 close to the surface, see also Figure 2b. The qualitative explanation is as follows: in [1], the discharge was run at lower pressure of gas mixture, 2 mbar, and line profiles were recorded from the whole HC cross-section with 1:6 optical reduction. Therefore, the reported profiles [1] represent an average value.

Here, an attempt is made to explain the large difference in G_3 radial distribution for HCDG operated in H_2 and Ar–H_2 mixture, see Figures 2 and 3. The largest difference relevant for G_3 comes from the cross-section data for excitation of the H_α line in a collision of a fast hydrogen atom H_f with the matrix gas, H_2 or Ar. All other collision excitation processes for the H_α excitation are negligible, see [17,18]. In the H_f energy range from 75 eV to 178 eV, the cross-sections for collision with Ar are between 82 and 8.5 times larger [17,18]. A large cross-section for the $H_f + Ar \rightarrow H^*$ collision explains larger G_3 values in Ar–H_2 mixtures in comparison with pure H_2. Furthermore, large cross-sections in Ar for lower H_f energies may be used to explain an increase of G_3 close to the HC surface. Namely, the backscattered H atoms from the HC surface in Ar–H_2 are still very efficient for the H_α excitation, which increases the G_3 value in the surface vicinity, see Figures 2b and 3b.

In order to test whether the HC temperature influences radial distributions of the Ar I and Ar II line intensities in SS and Ti HC operated with Ar–H_2 mixture, several experiments were carried out with the Ar I 420.07 nm and Ar II 427.75 nm lines. The summarized results are presented in Figure 4. For both cathode materials, the atomic line intensities decrease with temperature while ionic line increases with HC temperature. This effect is much more apparent in the case of Ti HC. Unfortunately, the reported results of a recent theoretical and experimental study of copper HC [19] were performed under different HCGD conditions in pure argon, and thus a sensible comparison cannot be made. However, the radial distribution change of Ar I and Ar II lines with HC temperature presented in Figure 4 suggests that HC temperature is one more parameter required for the HCGD modeling. It should be mentioned here that the importance of cathode temperature for some analytical GD applications has been discussed already in a number of publications, see e.g. [20–22].

In order to assess the influence of H_2 in Ar on the radial distribution of argon lines an experiment is carried out in pure Ar and in Ar–H_2 mixture and the results are given in Figure 5. To compare line intensity measurements in pure argon and gas mixture it was necessary to normalize intensities to the same voltage, which also implies the same electric power input since experiments are run with a constant current of 90 mA. The results in Figure 5 illustrate that, in the presence of 0.8% of H_2, the intensity of the Ar I line is considerably increased, while the intensity of the Ar II line rises too, but to a lesser extent. These and HC temperature dependences require further detailed studies, which are out of the scope of this work. It should

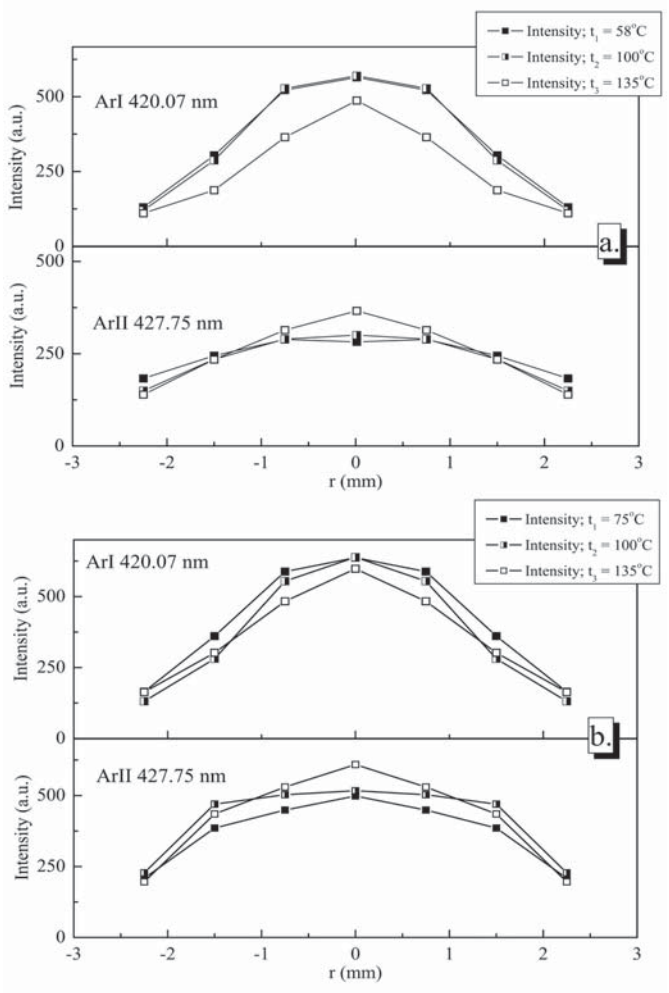

Fig. 4. Radial intensity distribution of neutral argon line Ar I 420.07 nm and singly ionized argon line Ar II 427.75 nm for different hollow cathode temperatures. Experimental conditions: (a) stainless steel cathode; for other experimental conditions see Table 2; (b) titanium cathode; for other experimental conditions see Table 4.

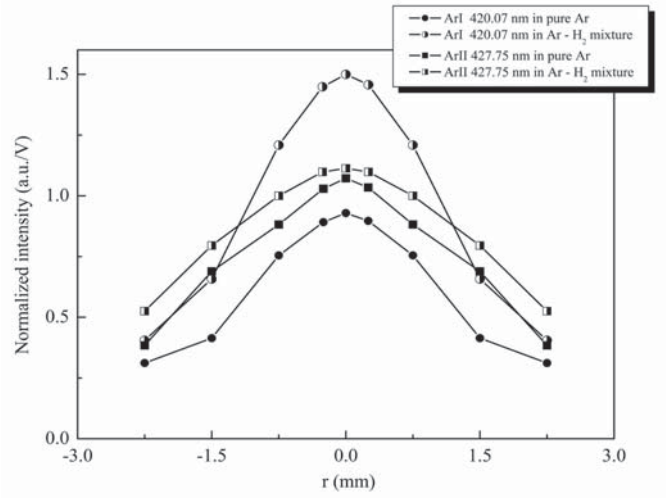

Fig. 5. Influence of hydrogen admixture on radial intensity distributions of neutral argon line Ar I 420.07 nm and single ionized argon line Ar II 427.75 nm. Discharge conditions: stainless steel cathode, discharge in pure Ar at $p = 4$ mbar; $I = 90$ mA; $U = 334$ V; $T_{wall} = 69$ °C; and in Ar–H_2 mixture at $p = 4$ mbar; $I = 90$ mA; $U = 300$ V; $T_{wall} = 55$ °C.

be pointed out that the influence of a small addition of H_2 in Ar is studied theoretically [23] and experimentally in Ar [24] and Ne [25] in some details using plane cathode abnormal glow discharge of the Grimm type.

It is interesting to notice that similar line shapes of the H_α and D_α lines, see Figure 1a and [11], are detected close to the first wall and in plasma diverters of large plasma fusion devices, see e.g. [26–29] and references therein. Although in these cases Doppler broadening is combined with the Zeeman line splitting, the same elementary atomic and molecular collisions and interaction with the wall surface are also present. Therefore, the shape of the Balmer lines in high temperature plasma reactors must bear certain resemblance to those reported here. On the other hand, simple devices like HCGD may be used for material testing and for study of elementary processes relevant for large plasma devices.

4 Conclusions

An experimental study of the excessively broadened part G_3 of the Balmer alpha line in HCGD operated with H_2 and Ar–H_2 gas mixture with SS or Ti cathodes shows considerably different radial distribution depending upon the choice of operating gas. The differences between radial G_3 distribution with SS and Ti cathode are evident, see Figures 2 and 3, and an increase with the HC temperature is always detected, see Tables 1–4. The increase of the excessively broadened part of the line profile is qualitatively explained with the help of back scattering coefficients for SS and Ti. The increase of the EDB part with HC temperature rise is related to metal hydride destruction at the cathode surface. A larger contribution of the excessively broadened part of the H_α line in Ar–H_2 in comparison with pure H_2 is explained in terms of the larger cross-section for the H_α excitation in the $H_f + Ar \rightarrow H^*$ reaction.

The influence of cathode temperature on the Ar I and Ar II line intensities is also detected by observing radial distributions of two argon lines. These results are only an indication of effect and further study of temperature behavior for a large number of spectral lines is required. Similar conclusions can be drawn from a study of the influence of H_2 traces in argon, see Figure 5.

The donation of a 2 m spectrometer from Dr. Volker Hoffmann, Leibniz-Institut für Festkörper- und Werkstoffforschung (IFW), Dresden, Germany, is gratefully acknowledged. This work within the Project 141029B "Low-temperature plasmas and gas discharges: radiative properties and interaction with surfaces" is supported by the Ministry of Science and Environmental Protection of the Republic of Serbia.

References

1. N. Konjević, G.Lj. Majstorović, N.M. Šišović, Appl. Phys. Lett. **86**, 251502 (2005)
2. B.M. Obradović, M.Sc. thesis, University of Belgrade (2001), in Serbian
3. N. Cvetanović, M.M. Kuraica, N. Konjević, J. Appl. Phys. **97**, 033302 (2005)
4. Z.Lj. Petrović, B.M. Jelenković, A.V. Phelps, Phys. Rev. Lett. **68**, 326 (1992)
5. M. Gemišić-Adamov, B.M. Obradović, M.M. Kuraica, N. Konjević, IEEE Trans. Plasma Sci. **31**, 444 (2003)
6. S.B. Radovanov, K. Dzierzerga, J.R. Roberts, J.K. Ollthoff, Appl. Phys. Lett. **66**, 2637 (1995)
7. I.R. Videnović, N. Konjević, M.M. Kuraica, Spectrochim. Acta **51B**, 1707 (1996)
8. R.L. Mills, P.C. Ray, B. Dandapani, R.M. Mayo, J. He, J. Appl. Phys. **92**, 7008 (2002)
9. R.L. Mills, P.C. Ray, M. Nansteel, X. Chen, R.M. Mayo, J. He, B. Dandapapanii, IEEE Trans. Plasma. Sci. **31**, 338 (2003)
10. A.V. Phelps, J. Appl. Phys. **98**, 066108 (2005)
11. `NotesOnMills.pdf` may be requested from `avp@jila.colorado.edu`
12. N.M. Šišović, G.Lj. Majstorović, N. Konjević, Eur. Phys. J. D **32**, 347 (2005)
13. C. Barbeau, J. Jolly, J. Phys. D **23**, 1168 (1990)
14. M. Warrier, R. Schneider, X. Bonnin, Computer Phys. Comm. **160**, 46 (2004)
15. T. Tabata, R. Ito, Present status of data compilation on ion backscattering, Institute of Plasma Physics Report, Nagoya, Japan, IPPJ-AM-64:84–89, 1989.
16. O.S. Oen, M.T. Robinson, J. Nucl. Mater. **76-77**, 370 (1978)
17. A.V. Phelps, J. Phys. Chem. Ref. Data **19**, 653 (1990)
18. A.V. Phelps, J. Phys. Chem. Ref. Data **21**, 883 (1992)
19. A. Bogaerts, A. Okhrimovskyy, N. Baguer, R.Gijbels, Plasma Sources Sci.Technol. **14**, 191 (2005)
20. S.K. Ohorodnik, W.W. Harrison, J. Anal. Atom. Spectr. **9**, 991 (1994)
21. M. Kasik, C. Michellon, L.C. Pitchford, J. Anal. Atom. Spectr. **17**, 1398 (2002)
22. A. Bogaerts, R. Gijbels, J. Anal. Atom. Spectrom. **18**, 1206 (2004)
23. A. Bogaerts, J. Anal. Atom. Spectrom. **17**, 768 (2002)
24. V.-D. Hodoroaba, V. Hoffmann, E.B.M. Steers, K. Wetzig, J. Anal. Atom. Spectrom. **15**, 1075 (2000)
25. V.D. Hodoroaba, E.B.M. Steers, V. Hoffmann, K. Wetzig, J. Anal. Atom. Spectrom. **16**, 43 (2001)
26. J.D. Hey, C.C. Chu, E. Hintz, Contrib. Plasma Phys. **40**, 9 (2000)
27. M. Koubiti, Y. Marandet, A. Escarguel, H. Capes, L. Godbert-Mouret, R. Stamm, C. De Michelis, R. Guirlet, M. Mattioli, Plasma Phys. Control. Fusion **44**, 261 (2002)
28. J.D. Hey, C.C. Chu, Ph. Mertens, S. Brezinsek, B. Unterberg, J. Phys. B: At. Mol. Opt. Phys. **37**, 2543 (2004)
29. J.D. Hey, C.C. Chu, Ph. Mertens, J. Phys. B: At. Mol. Opt. Phys. **38**, 3517 (2005)